Vol 12 No 2, February 2003
1009-1963/2003/12(02)/0169-05

Chinese Physics

A theoretical study about the chirped pulse amplification laser*

Lu Xing-Qiang(卢兴强) and Fan Dian-Yuan(范滇元)

State Key Laboratory on High Power Laser and Physics, Shanghai Institute of Optics and Fine Mechanics, Chinese Academy of Sciences, Shanghai 201800, China

(Received 21 June 2002; revised manuscript received 14 August 2002)

Starting from the Maxwell's equation, and using the resonant-dipole equation together with the multilevel rate equations which take the effects of energy relaxation into consideration, we have derived a more realistic numerical model of the chirped pulse amplification for an ultra-broad band width laser amplifier. Numerical simulations of this model show that both the intensity profile and the energy fluence of the amplified chirped pulse are closely connected with the two relaxation effects: the relaxation of the thermalization among the components of the laser multiplets and the depletion of the lower laser level. The results are valuable for the design of ultra-broad bandwidth chirped pulse amplification lasers.

Keywords: chirped pulse amplification, Maxwell's equation, relaxation of energy level
PACC: 4210, 4255, 4260

1. Introduction

Ultra-short pulse lasers with high-peak-power are applicable in many fields, such as fusion, plasma physics, x-ray generation, and so on.[1,2] However, the construction of high-power ultra-short pulse lasers is a kind of long-term and high-technique work, whose key problem is to guarantee the quality of the laser amplification and reduce the expense. In this case, the corresponding theoretical study can provide proper parameters for the laser-building, and help to optimize the system and decrease the difficulty of the laser-building. For the chirped pulse amplification (CPA)[3] is an effective regime to produce ultra-short high-peak-power lasers in solid-state laser medium, and the characteristics of pulses under different conditions can all be described by the definition of the chirped pulse.[4] Thus in this paper, we make a theoretical study about CPA in detail.

Two types of theoretical model for CPA have been reported so far. One is the coherent amplification model,[5] which is derived from the Maxwell's equation, the resonant-dipole equation and the rate equations. The other is based on the ordinary Frantz–Nodvik model,[6] which uses the transport equation and the rate equations to describe the propagation of chirped pulses.[7,8] We should note that the self-phase modulation and dispersion are considered in the former model. This model can describe the characteristics of a CPA laser more accurately and is used more frequently than the latter model,[9,10] which is a reduction of the former.[11] The coherent amplification model has been reported in Ref.[5], however, a narrow bandwidth approximation has also been introduced into it to investigate the amplification properties of Nd:glass, which has a relatively narrower bandwidth. Therefore, the model in Ref.[5] cannot be used to investigate the amplification characteristics of the ultra-broad bandwidth laser medium, e.g. the main gain medium of the CPA Ti:sapphire laser. In this paper, the model in Ref.[5] will be extended, and another coherent amplification model will be derived. In this case, the narrow bandwidth approximation used in Ref.[5] is eliminated, while the multilevel rate equations,[12] including the effects of the energy relaxation, are introduced into it. To the best of our knowledge, this is the most realistic coherent amplification theoretical model for the CPA laser.

2. Theoretical model

If an amplifier is placed within the Rayleigh range of a light beam, and the transverse 00 mode of the

*Project supported by the National High Technology Inertial Confinement Fusion Foundation of China (Grant No 863-804-5).

pulse keeps invariable when the light is amplified, the propagation of a pulse in an amplifier can be described by the Maxwell's equation[4,5]

$$\begin{aligned}&\frac{\partial^2 \boldsymbol{E}(z,t')}{\partial z^2}-\frac{1}{c_0^2}\frac{\partial^2 \boldsymbol{E}(z,t')}{\partial t'^2}\\&=\mu_0\frac{\partial^2}{\partial t'^2}[\boldsymbol{P}_{\rm L}(z,t')+\boldsymbol{P}_{\rm NL}(z,t')+\boldsymbol{P}(z,t')],\end{aligned}\quad(1)$$

where $\boldsymbol{E}(z,t')$ is the electric field, z is the propagation distance, t' is the time in the laboratory time frame, c_0 is the speed of light in vacuum, μ_0 is the permeability in vacuum, $\boldsymbol{P}(z,t')$ is the resonant polarization of the gain medium, and $\boldsymbol{P}_{\rm L}(z,t')$ and $\boldsymbol{P}_{\rm NL}(z,t')$ are the linear and nonlinear polarizations of the gain medium, respectively, which satisfy

$$\begin{cases}\boldsymbol{P}_{\rm L}(z,\omega)+\varepsilon_0\boldsymbol{E}(z,\omega)=n_{\rm L}^2(\omega)\varepsilon_0\boldsymbol{E}(z,\omega),\\ \boldsymbol{P}_{\rm NL}(z,t')=2n_0n_{2\rm E}<\boldsymbol{E}^2(z,t')>\varepsilon_0\boldsymbol{E}(z,t').\end{cases}\quad(2)$$

Here $\boldsymbol{P}_{\rm L}(z,\omega)$ and $\boldsymbol{E}(z,\omega)$ are the Fourier transforms of the $\boldsymbol{P}_{\rm L}(z,t')$ and $\boldsymbol{E}(z,t')$, respectively, $n_{\rm L}(\omega)$ is the linear index of the refraction, $n_0=n_{\rm L}(\omega_0)$ is the linear index of the refraction at the carrier frequency ω_0, $n_{2\rm E}$ is the coefficient of the nonlinear index of the refraction.

In the homogeneously broadened multilevel gain medium, the resonant polarization $\boldsymbol{P}(z,t')$ is governed by the resonant-dipole equation[4,5]

$$\begin{aligned}&\frac{\partial^2 \boldsymbol{P}(z,t')}{\partial t'^2}+\Delta\omega_{\rm a}\frac{\partial \boldsymbol{P}(z,t')}{\partial t'}+\omega_{\rm a}\boldsymbol{P}(z,t')\\&=-K[N_2(z,t')-N_1(z,t')]\boldsymbol{E}(z,t'),\end{aligned}\quad(3)$$

where $\Delta\omega_{\rm a}$ is the spectral width of the gain medium (FWHM), $\omega_{\rm a}$ is the centre angular frequency of the spectral, $N_2(z,t')$ and $N_1(z,t')$ are the population density of the upper and lower lasers levels respectively, $K=\varepsilon c\sigma_0\Delta\omega_{\rm a}$ is a constant, in which ε, c and σ_0 are the permittivity of the gain medium, the speed of light in the gain medium, and the stimulated cross section of the gain medium at $\omega_{\rm a}$, respectively.

Neglecting the influence of the pump during the amplification, the more realistic multilevel rate equations can be written as follows[12]

$$\begin{aligned}\frac{\partial N_2(z,t')}{\partial t'}=&-W_{21}[N_2(z,t')-N_1(z,t')]\\&+\frac{N_2'(z,t')-k_2N_2(z,t')}{\zeta(1+k_2)}-\frac{N_2(z,t')}{\tau_2},\end{aligned}$$

$$\frac{\partial N_2'(z,t')}{\partial t'}=-\frac{1}{\zeta(1+k_2)}[N_2'(z,t')-k_2N_2(z,t')],$$

$$\begin{aligned}\frac{\partial N_1(z,t')}{\partial t'}=&W_{21}[N_2(z,t')-N_1(z,t')]\\&+\frac{N_1'(z,t')-k_1N_1(z,t')}{\zeta(1+k_1)}\\&+\frac{N_2(z,t')}{\tau_2}-\frac{N_1(z,t')}{\tau_1},\end{aligned}$$

$$\frac{\partial N_1'(z,t')}{\partial t'}=-\frac{1}{\zeta(1+k_1)}[N_1'(z,t')-k_1N_1(z,t')],\quad(4)$$

where $N_2(z,t')$ and $N_2'(z,t')$ are two multiplets of the upper energy level, $N_1(z,t')$ and $N_1'(z,t')$ are two multiplets of the lower energy level (stimulated transition occurs between the laser levels $N_2(z,t')$ and $N_1(z,t')$), τ_2 and τ_1 are lifetimes of the upper and the lower laser levels, k_2 and k_1 are the coefficients of the Boltzmann distribution for the upper and the lower energy levels, respectively. ζ is the thermalization time, $\hbar$ is the Planck's constant, and W_{21} is the possibility of the stimulated transition of the upper laser level, which is governed by,[4,5,11]

$$W_{21}[N_2(z,t')-N_1(z,t')]=\frac{1}{\hbar\omega_{\rm a}}\boldsymbol{E}(z,t')\cdot\frac{\partial \boldsymbol{P}(z,t')}{\partial t'}.\quad(5)$$

Equations (1)–(5) are the basic equations to describe the chirped pulse propagation in a laser amplifier. When $\boldsymbol{E}(z,t')$, $\boldsymbol{P}(z,t')$, $\boldsymbol{P}_{\rm L}(z,t')$ and $\boldsymbol{P}_{\rm NL}(z,t')$ are polarized in the same direction, these equations can be simplified by dropping their vector notation, which is made as follows

$E(z,t')$ and $P(z,t')$ can be written as

$$\begin{cases}E(z,t')={\rm Re}\{E_0(z,t'){\rm exp}[{\rm i}(\omega_0t'-\beta_0z)]\},\\ P(z,t')={\rm Re}\{P_0(z,t'){\rm exp}[{\rm i}(\omega_0t'-\beta_0z)]\},\end{cases}\quad(6)$$

where $\beta_0=n_0\omega_0/c$ is the propagation constant at the carrier frequency ω_0. The frequency-dependent propagation constant can be expanded as

$$\begin{aligned}\beta(\omega)=&\frac{\omega n_{\rm L}(\omega)}{c}\\\approx&\beta_0+\beta'(\omega-\omega_0)+\frac{1}{2}\beta''(\omega-\omega_0)^2,\end{aligned}\quad(7)$$

where β' and β'' are the first-and the second-order derivatives of the $\beta(\omega)$ evaluated at ω_0. Then following the simplification steps in Ref.[13], substituting Eqs.(2), (3) and (6) into Eq.(1), and by using the slowly varying envelope approximation (SVEA) and the dispersion expression (7), we obtain

$$\begin{aligned}&\frac{\partial E_0(z,t')}{\partial z}+\beta'\frac{\partial E_0(z,t')}{\partial t'}\\&=-{\rm i}\frac{\omega_0}{2\varepsilon c}P_0(z,t')+{\rm i}\frac{\beta''}{2}\frac{\partial^2E_0(z,t')}{\partial t'^2}\\&\quad-{\rm i}\frac{\beta_2}{2}|E_0(z,t')|^2E_0(z,t'),\end{aligned}\quad(8)$$

where $\beta' = 1/3$, $\beta_2 = 2\pi n_{2E}/\lambda_0$, with λ_0 being the wavelength in vacuum. Similarly, applying SVEA to Eq.(3) and dropping the second harmonic (or 2ω) terms in Eq.(5), we have

$$\begin{aligned}&\frac{\partial P_0(z,t')}{\partial t'}\\ =&-\frac{1}{\Delta\omega_a+\mathrm{i}2\omega_0}[(\mathrm{i}\omega_0\Delta\omega_a-\omega_0^2+\omega_a^2)P_0(z,t')\\ &+K[N_2(z,t')-N_1(z,t')]E(z,t')],\end{aligned}\tag{9}$$

$$\begin{aligned}&W_{21}[N_2(z,t')-N_1(z,t')]\\ =&-\mathrm{i}\frac{\omega_0}{4\hbar\omega_a}[E_0^*(z,t')P_0(z,t')-E_0(z,t')P_0^*(z,t')].\end{aligned}\tag{10}$$

We should stress that Eqs.(4), (8), (9) and (10) are the components of the coherent amplification model for the CPA laser in ordinary laboratory time frame. Before making numerical simulation of them, the moving time frame $t = t' - \beta' z$ should be introduced into the equation, so we obtain

$$\begin{aligned}\frac{\partial E_0(z,t')}{\partial z}=&-\mathrm{i}\frac{\omega_0}{2\varepsilon c}P_0(z,t)+\mathrm{i}\frac{\beta''}{2}\frac{\partial^2E_0(z,t)}{\partial t^2}\\ &-\mathrm{i}\frac{\beta_2}{2}|E_0(z,t)|^2E_0(z,t),\end{aligned}$$

$$\begin{aligned}&\frac{\partial P_0(z,t)}{\partial t}\\ =&-\frac{1}{\Delta\omega_a+\mathrm{i}2\omega_0}\{(\mathrm{i}\omega_0\Delta\omega_a-\omega_0^2+\omega_a^2)P_0(z,t)\\ &+K[N_2(z,t)-N_1(z,t)]E(z,t)\},\end{aligned}$$

$$\begin{aligned}\frac{\partial N_2(z,t)}{\partial t}=&-W_{21}[N_2(z,t)-N_1(z,t)]\\ &+\frac{N_2'(z,t)-k_2N_2(z,t)}{\zeta(1+k_2)}-\frac{N_2(z,t)}{\tau_2},\end{aligned}$$

$$\frac{\partial N_2'(z,t)}{\partial t}=-\frac{1}{\zeta(1+k_2)}[N_2'(z,t)-k_2N_2(z,t)],$$

$$\begin{aligned}\frac{\partial N_1(z,t)}{\partial t}=&W_{21}[N_2(z,t)-N_1(z,t)]\\ &+\frac{N_1'(z,t)-k_1N_1(z,t)}{\zeta(1+k_1)}\\ &+\frac{N_2(z,t)}{\tau_2}-\frac{N_1(z,t)}{\tau_1},\end{aligned}$$

$$\frac{\partial N_1'(z,t)}{\partial t}=-\frac{1}{\zeta(1+k_1)}[N_1'(z,t)-k_1N_1(z,t)],$$

$$\begin{aligned}&W_{21}[N_2(z,t')-N_1(z,t')]\\ =&-\mathrm{i}\frac{\omega_0}{4\hbar\omega_a}[E_0^*(z,t)P_0(z,t)-E_0(z,t)P_0^*(z,t)].\end{aligned}\tag{11}$$

Equations (11) are the numerical coherent amplification model for the CPA laser. They have two advantages compared with that in Ref.[5]; one is that no narrow bandwidth approximation ($\Delta\omega_a \ll \omega_a$) is introduced, so that it can be used to investigate the amplification characteristics of an ultra-broad bandwidth gain medium; the other is that the multilevel rate equations used in Eqs.(11) can be easily simplified to the rate equations of two or three-level laser system by varying τ_1 and ζ,[12] i.e. Eqs.(11) are a more realistic amplification model for the CPA laser.

The final equation in Eqs.(11) can be further simplified using the expression $P_0(z,t) \approx \chi\varepsilon E_0(z,t)(\chi' + \mathrm{i}\chi'')\varepsilon E_0(z,t)$,[4] thus we have

$$\begin{aligned}&W_{21}[N_2(z,t)-N_1(z,t)]\\ \approx&\frac{1}{\hbar\omega_a}\frac{\omega_0}{c}\chi''(\omega)I(z,t)\\ =&\frac{1}{\hbar\omega_a}\sigma(\omega)N(z,t)I(z,t).\end{aligned}\tag{12}$$

Equation (12) provides another numerical model for the CPA laser, by which we can use experimental data of the stimulated cross section $\sigma(\omega)$ to gain more realistic computer-simulated results.

3. Numerical simulations

The influences of the two energy relaxation effects will be demonstrated in detail in this section. We use, Nd:glass as the amplifier, and give its parameters as follows.[5,14,15] The centre wavelength λ_a=1053nm, the spectral width $\Delta\lambda_a$=30nm, the constants K_1=1.651, K_2=0.463, the saturation energy fluence $h\nu_a/\sigma_0$ is 4.7J·cm^{-2}, and the small-signal gain of the amplifier is 50. Furthermore, a fifth super-Gaussian chirped pulse is applied as the input signal, whose positive linear chirp amount is governed by $\Delta\omega_L\tau/2$,[5] in which $\Delta\omega_L = 2\pi c\Delta\lambda_L/\lambda_0^2$ is the spectral width of the input signal, τ is the half pulse width at e^{-1} intensity points. The parameters of the input signal are as follows: the centre carrier wavelength λ_0=1053nm, the spectral width $\Delta\lambda_L$=5nm, the half pulse width τ=1ns, and the input energy fluence is 0.19J·cm^{-2}.

3.1. Influences of the amplified chirped pulse on the intensity profile

There are two types of energy relaxation:[15] one is the depletion of the lower laser level, and the other is the thermalization among the components of the upper and lower energy multiplets. Both types of energy

relaxation can increase the decreased inverse population during the amplification of the pulse, but the mechanisms are different. The former increases the inverse population by decreasing the population of the lower laser level, while the latter increases the inverse population by spreading the population among the components of the energy multiplets under thermalization equilibrium condition. This makes no change to the total population of the upper and lower energy levels. Figures 1 and 2 show the influences of the two types of energy relaxation on the intensity profiles of the amplified chirped pulses, respectively.

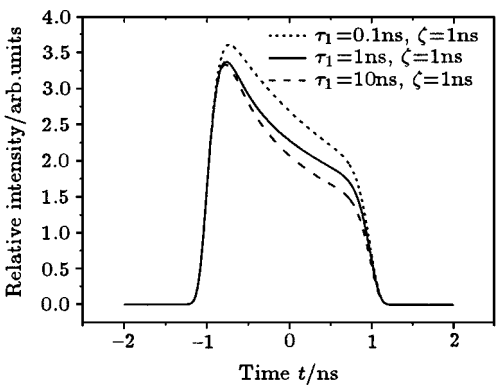

Fig.1. Intensity profiles of the amplified chirped pulse for different depletion time τ_1=0.1, 1 and 10ns at the same thermalization time ζ=1ns.

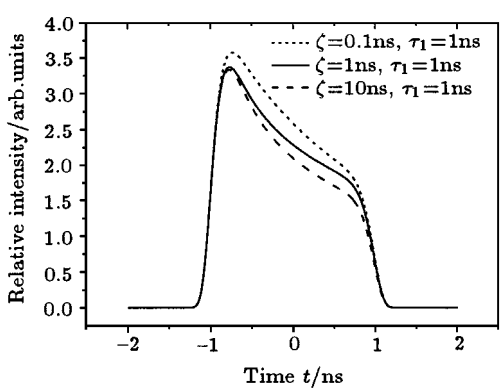

Fig.2. Intensity profiles of the amplified chirped pulse for different thermalization time ζ=0.1, 1 and 10ns, at the same depletion time τ_1=1ns.

Although the amplitudes of the two figures are different at the trailing edge of the pulses, both figures vary with the same tendency. The intensity of the chirped pulse increases with decreasing the relaxation time, and the influence of the gain saturation on the pulse is less when the relaxation time is shorter, i.e. for a shorter relaxation time with a higher relaxation rate, the decreased inverse population can be increased faster during the amplification, so the input pulse can be amplified to a higher intensity for its higher inversion population. On the contrary, when the relaxation time is longer, the relaxation rate is slower and the intensity of the amplified chirped pulse will be decreased due to the relative lower inverse population.

3.2. Influences on the energy fluence of the amplified chirped pulse

Figure 3 shows the influences of the energy relaxations on the energy fluence of the amplified chirped pulse.

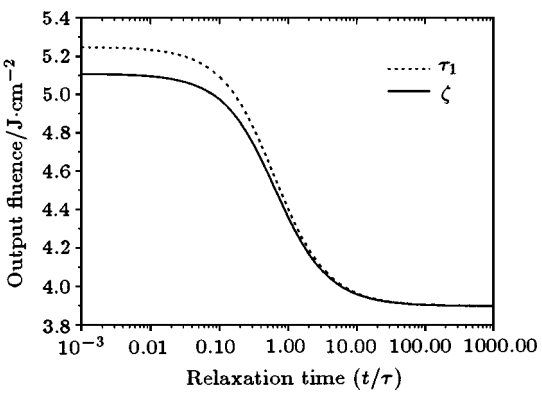

Fig.3. Output fluence of the amplified chirped pulse versus the thermalization time ζ and the depletion time τ_1.

We can see that for the same relaxation time, the output energy fluence of the amplified chirped pulse under the effect of the depletion (dashed line) is higher than that under the effect of the thermalization (solid line). This is just because the depletion decreases the population of the lower laser level, while the thermalization only redistributes the population of the lower and the upper energy levels, and the total population of them keeps unchanged. Thus, when the relaxation rates are equivalent, the depletion can increase the decreased inverse population more efficiently than the thermalization, and the pulse can have a better amplification with a higher output energy fluence under this condition.

In fact, the effects of both relaxations are coexisting in the laser amplifier and they would affect each other, which may be seen clearly in Fig.4.

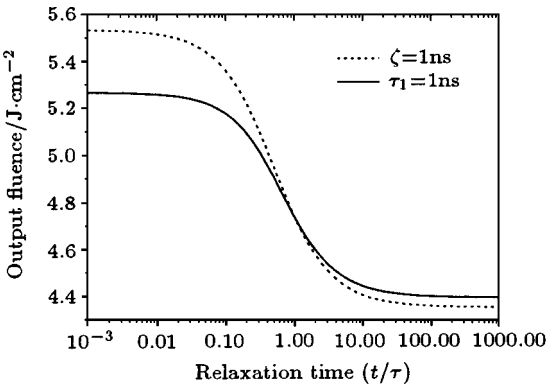

Fig.4. Influences of the depletion (dashed line with the same thermalization time ζ=1ns) and the thermalization (solid line with the same depletion time τ_1=1ns) on the output energy fluence of the amplified chirped pulse.

The dashed and solid lines in Fig.4 show the output energy fluence of the amplified chirped pulse versus the lifetime of the lower laser level and the thermalization time, respectively. It can be seen that both lines decrease when the relaxation time increases and the rapid variation of them occurs when the relaxation time is about equal to the width of the pulse. Furthermore, differing from those in Fig.3, the lines in Fig.4 are crossed at about 1ns under our calculation conditions. We should note that this kind of cross is caused by the competition of the two relaxation effects. When the relaxation time is shorter than 1ns, for the dashed line, the depletion plays the main role in increasing the inverse population for the depletion time is less than the thermalization time; but for the solid line, the depletion time is longer than the thermalization time on this condition, and the thermalization plays the main role in increasing the inverse population during the amplification. Since the depletion can increase the decreased inverse population more efficiently than the thermalization (Fig.3), when the relaxation time is shorter than 1ns, the dashed line is higher than the solid line, and the pulse can have a better amplification with a higher energy fluence. On the contrary, when the relaxation time is longer than 1ns, the roles of both relaxation effects will interchange in the two lines, i.e. the thermalization and the depletion will play the main role in increasing the decreased inverse population in the dashed and solid lines, respectively. As a result, the output fluence of the pulse in the dashed line will be lower than that in the solid line, and the two lines are crossed at about 1ns.

4. Summary

We have derived a numerical simulation model for the ultra-broad bandwidth CPA Laser. It is a more realistic model for designing high-power laser amplifiers since the multilevel rate equations are introduced into it. By performing a numerical simulation to the model, we have investigated in detail the influences of the relaxation of the depletion of the lower laser level and the thermalization among the components of the laser multiplets on the intensity profiles and energy fluences of the amplified pulse. The results give in this paper are valuable for choosing the parameters of the amplifier and simulating the amplification process of the high-power ultra-short laser amplifier systems.

References

[1] Perry M D and Mourou G 1994 *Science* **264** 917

[2] Xiao J, Wang Z Y and Xu Z Z 2001 *Chin. Phys.* **10** 941

[3] Strickland D and Mourou G 1985 *Opt. Commun.* **56** 219

[4] Siegman A E 1986 *Lasers* (Mill Valley, CA: University Science Books) ch 2, 4 ,5, 9 and 10

[5] Chuang Y H, Zheng L and Meyerhofer D D 1993 *IEEE J. Quantum Electron.* **29** 270

[6] Frantz L M and Nodvik J S 1963 *J. Appl. Phys.* **34** 2346

[7] Yamakawa K, Aoyama M, Matsuoka S *et al* 1998 *Opt. Lett.* **23** 1468

[8] Zhang S K, Wen G J, Zhou P Z *et al* 1996 *High Power Laser and Particle Beam* **8** 500 (in Chinese)

[9] Zhao S H, Wang Y S, Wang G F *et al* 1997 *Acta Photon. Sin.* **26** 197 (in Chinese)

[10] Shen Y Z, Wang Q Y, Xing Q R *et al* 1996 *Acta Phys. Sin.* **45** 211 (in Chinese)

[11] Lowdermilk W H and Murray J E 1980 *J. Appl. Phys.* **51** 2436

[12] Wang T and Fan D Y 1999 *Acta Opt. Sin.* **19** 468 (in Chinese)

[13] Agrawal G P 1989 *Nonlinear Fibre Optics* (Boston, MA: Academic) chap 2

[14] Linford G J, Saroyan R A, Trenholme J B *et al* 1979 *J. IEEE J. Quantum Electron.* **15** 510

[15] Fan D Y and Yu W Y 1980 *Chin. J. Lasers* **7** 1 (in Chinese)